JNBT
©2008INBDK

JNBT, Vol 4, No 1, pp. 19-26

Optical transition studies of semiconductor quantum structures in high magnetic fields

Yongmin Kim

Department of Applied Physics and Institute of Nanosensor and Biotechnology,
Dankook University, Yongin 448-701, Korea

ABSTRACT

Semiconductors are characterized not only by their energy gaps but also by various impurity energy levels. These energy levels are well organized by optical transition studies. For a semiconductor heterostructure wherein two different semiconductors are attached, a quantum structure with distinguished new energy levels are obtained. Photoluminescence spectroscopy in magnetic fields at low temperatures has proved to be a powerful technique for investigating the electronic states of quantum semiconductor heterostructures and offers a complimentary tool to electrical transport studies. We have undertaken a comprehensive investigation of magneto-excitonic and Landau transitions in a large variety of undoped and doped quantum-well structures. A broad range of samples have been investigated in high magnetic fields as a function of temperature, sample geometry, and high pressure. Examples include single and coupled double quantum wells, modulation-doped quantum wells, and single interface heterojunction structures.

Key words : magnetic field, semiconductor quantum well, photoluminescence, exciton, quantum Hall effect

Introduction

A simplest quantum confined structure of semiconductors can be achieved by attaching two different semiconductors with different energy band gap. Deposition of two different semiconductor layers (typically <100 Å) repeatedly, a completely new type of two-dimensional (2D) carrier properties can be established. Such low dimensionality exhibits noble properties as integer (1) and fractional (2) quantum Hall effects, quantum confined stark effect, and so on. Optical spectroscopy at low temperature (typically below 4 K) and high magnetic fields has proved to be a powerful tool for investigating the ground and excited states of high-quality quantum-well-type 2D semiconductor heterostructures (3) because optical transitions are strongly influenced by electron-electron interactions and the method offers a complimentary tool to electrical transport studies.

* Corresponding author :
Yongmin Kim
Tel : +82-31-8005-3209
Fax : +82-31-8005-3208
E-mail : yongmin@dankook.ac.kr

Generation of High Magnetic Fields

Continuous magnetic fields can be achieved to 21 tesla (T) and 33 T using superconducting and resistive magnets, respectively. In comparison, the average magnetic field of the earth is about 5×10^{-5} T. Since superconducting wires are used for a solenoid type electrical magnet, large amount of liquid helium (LHe^4) is consumed to maintain superconducting properties of the solenoid. On the other hand, a resistive magnet uses multiple of copper plate to construct a solenoid. In this case, large amount of electricity and deionized cooling water is required. To generate more than 30 T, pulsed magnet systems are widely used. Normally, capacitor bank systems are used for which large amount of charges are stored in capacitors and discharged in a short period of time

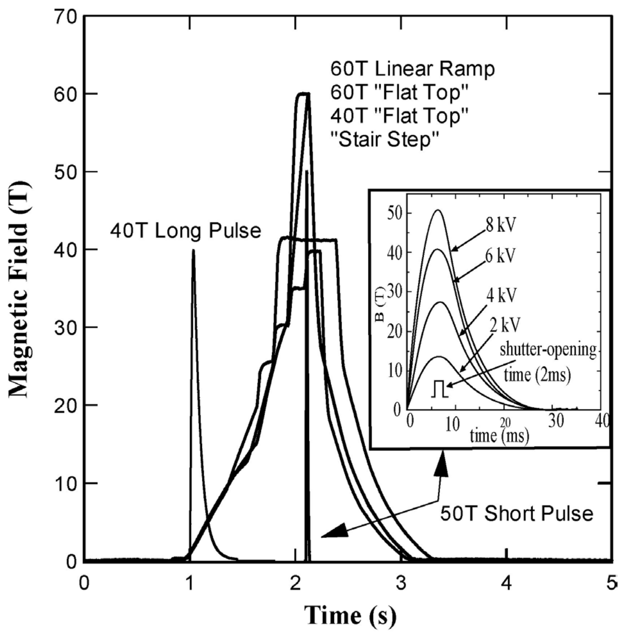

Fig 1. Pulsed magnetic field profiles. Capacitor-driven short pulse magnet has only 25 ms transient time and a optical spectrum can be taken once at the top the field for 2 ms during the pulse (see inset). Capacitor-driven mid pulse magnet has ~ 0.5 s field duration and optical measurements can be made continuously at every 2 ms spectrum acquisition time during the pulse using charge coupled device (CCD) detrctor. Power generator-driven long pulse magnet has 2 s fields duration and also various pulse modes are available.

(30ms ~ 0.5s) to a magnet. The highest and meaningful magnetic field for physical experiments for a capacitor - driven pulsed magnet is around 60 T along with ~ 25 ms transient time of the field. To enlarge the transient time, a power-generator driven long pulse magnet is used which generates magnetic fields as high as 60 T during 2 s transient time (see Fig 1). The virtue of long pulse magnet is to reduce eddy current heating. When a metallic sample located in time-varying magnetic fields, an eddy current is induced which proportional to the time derivative of magnetic field (dB/dt). Consequently, fast-varying pulsed magnetic fields generate large eddy current induced heating to any conducting materials which deteriorate low temperature properties of samples. The advent of power generator driven long pulse magnet system made it possible to measure low temperature properties of conducting samples. A liquid ^{4}He flow cryostat (~1.5 K) and a liquid ^{3}He (~0.5 K) refrigerator are employed to maintain low temperature in a liquid ^{4}He bath dewar.

Physical Properties of Low Dimensional Semiconductors

At low temperature, there exist many sources of bound state charges. For example, an ionized donor attracts an electron to consist a hydrogen-like structure. An electron and a hole also construct a hydrogen-like structure, so called an exciton (X). For a direct band gap intrinsic semiconductor, external excitation such as laser light can excite electrons in the valence band to the conduction band leaving holes behind. Such electron-hole pairs form excitons. It is expected that ionized hydrogen-like charged exciton structures such as two electrons bound to a hole (X^-) or two holes with an electron (X^+) are able to be formed (4). In a bulk (3D) semiconductor crystal, due to the small binding energy of charged excitons, it is difficult to detect them. However, in 2D quantum wells, binding energies of charged excitons are detectably enhanced (5). In the presence of magnetic field, when a charged exciton satisfies the selection rule of $\triangle S=\pm 1$ where S is spins of particles, they recombine and generate a photon with right or left circular polarization (RCP, LCP).

For a doped semiconductor, due to the screening within the majority carriers, Coulomb attraction between free electrons and free holes are negligible. As a consequence, in a doped semiconductor, formation of excitonic structures is prevented. In this case, a simple free carrier recombination is detected. The main difference between exciton and free carrier recombination is the amount of transition energy. Normally, a free carrier transition energy (E) is the same as the band gap (E_g) of the given semiconductor whereas an exciton transition energy differs the amount of binding energy (E_b) from the band gap, $E=E_g-E_b$. Exciton binding energies vary from~5 meV (GaAs) to~60 meV (ZnO) depending on materials. Therefore, GaAs can not form excitons at room temperature while excitons in ZnO survive above the room temperature. In the presence of magnetic field, excitons undergo simple diamagnetic energy shift ($E=\varepsilon^2\hbar^4B^2/4e^2\mu^3$) and free carriers undergo cyclotron motion and its energy quantized. The quantized cyclotron energy level known as Landau level is,

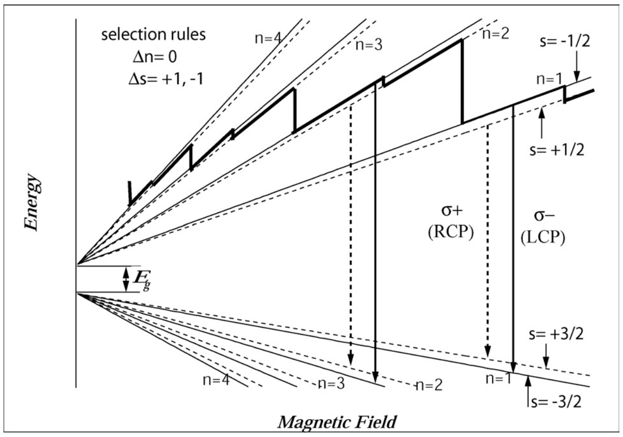

Fig 2. Formation of Landau levels in magnetic fields. Two selection rules for optical transitions are depicted. Selection rule for Landau level transition is $\Delta n = n_{\text{conduction band}} - n_{\text{valence band}} = 0$. Each Landau level splits two spin levels which are ±1/2 for conduction electrons and ±3/2 for valence holes. Solid arrow and dashed arrow indicate left circularly polarized (LCP) and right circularly polarized (RCP) photons after recombinations. Thick solid line exhibits the oscillating behavior of the Fermi energy with increasing magnetic fields. When the Fermi energy jump from higher to lower Landau levels, the integer quantum Hall effect occurs.

$$E_n = \left(n + \tfrac{1}{2}\right)\hbar \frac{eB}{m} = \left(n + \tfrac{1}{2}\right)\hbar\omega_c \tag{1}$$

where n, e, m, and B are integer numbers, electric charge, electron mass and external magnetic field, respectively, and $\omega_c = eB/m$ is known as cyclotron frequency. From this equation, we know that the carriers obtain quantized magnetic energy which is proportional to external magnetic fields. However, in specific magnetic fields, due to the strong correlations within 2D free carriers, optical and transport phenomena exhibit integer and fractional quantum Hall effects.

We have measured a magneto-optical properties of semiconductor quantum structures using fiber optic probes to switch between steady state (to 18 T) and pulsed (to 65 T) magnetic fields applied perpendicular (Faraday geometry, $\boldsymbol{B}\perp z$) and parallel (Voigt geometry, $\boldsymbol{B}/\!/z$) to the growth axis of the 2D layers. We have studied both modulation-doped and undoped quantum wells and single interface structures (6). At low magnetic fields (15 T) the magneto-photoluminescence (MPL) spectral data for undoped GaAs-AlGaAs single quantum wells (SQWs) show a diamagnetic shift characteristic of magneto-excitons; at high fields (~35 T), the shift becomes linear (7). In the vicinity of 25 T, all undoped QW samples exhibit anti-crossing of the heavy and light hole excitons (8) due to valence band mixing effects (9). Landau transitions corresponding to band to band recombination are observed in all modulation-doped GaAs-AlGaAs and InGaAs-GaAs single and multiple quantum well structures. Large non-linear effects are observed in the energy and the intensity versus magnetic field as Landau levels in the conduction band cross the Fermi level (10-12). In a modulation-doped single heterojunction (SHJ), photogenerated electrons play an important role as they can easily transfer into the triangular shaped well at the interface (13-15). Minima in the PL with magnetic field correspond to maxima in the PL intensity. This anomalous MPL behavior with magnetic field is confirmed in complementary optical Shubnikov-de Hass measurements. The oscillatory behavior in both the optical and transport data agree well with self-consistent calculation of the variation in the second subband carrier density (16, 17). We have made a series of measurements of a modulation-doped InGaAs-GaAs SQW a function of pressure from 0-3.5 GPa at 4 and 77 K in fields up to 50 T. At 77 K, the allowed 0-0, 1-1, 2-2, Landau transitions are dominant; at 4 K, in addition to the 0-0, we observe the forbidden transitions 0-1, 0-2, etc. in agreement with ambient pressure, 0-15 T studies in Refs (18-19). In the 4 K data, intensity and energy anomalies were found similar to those observed by others (10-13). At about 25 T there was a discrete reduction in the slope of the 0-0 transition. Apart from the predicted shift associated with the band gap, no unusual variations in the energy or intensity with pressure were found (19, 20).

Experimental

The spectroscopic measurements have been made at the National High Magnetic Field Laboratory, Los Alamos National Laboratory (NHMFL-LANL), Pulsed Field Facility. MPL measurements were performed at 4 and 77 K up to 18 T in a superconducting magnet and to 50/65 T in a pulsed magnet. A block diagram of the optical set-up for the MPL measurements using

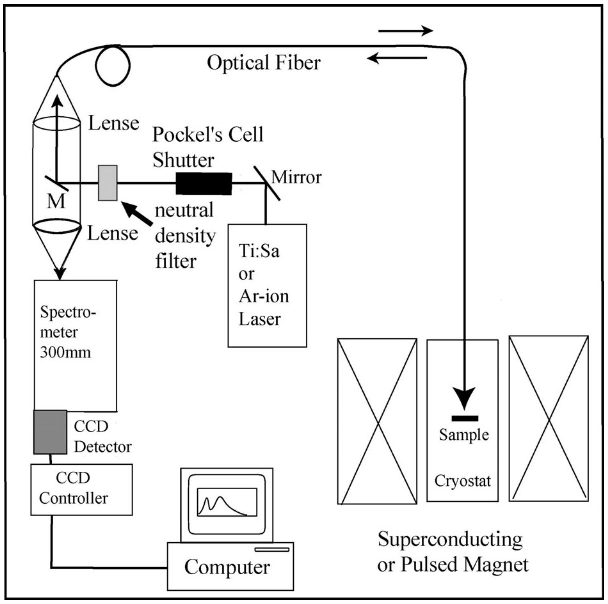

Fig 3. Experimental set up for optical spectroscopic measurements. A multi-mode optical fiber carries laser light to and photoluminescence signal from the sample located at the center of the magnet. Fast CCD detector system made it possible to take a PL spectrum at every 2 ms during transient magnetic fields.

an liquid nitrogen cooled CCD array detector is shown in Fig 3. The pulse profiles for various pulsed-magnets at NHMFLLANL are shown in Fig 1. For a short pulse magnet, the Pockels cell shutter was set to open for 2 ms corresponding to the flat-top region at the peak of the field. The spectra were recorded during this time interval. The spectral range depended on the grating selected in the spectrograph; data were usually taken with a spectral resolution of ~0.05 meV. The excitation energy was provided by individual lines from an 10 W Ar^+ laser or an Ar^+-pumped Ti-sapphire laser (tunable from 700-1050 nm). Different fiber optic probes (140-600 ㎛ diameter) were available. A multimode optical fiber was used as both an input and an output coupler. The sample holder was attached directly to the end of the fiber bundle for easy selection of fiber diameter, DC or pulsed magnet field, or field direction (perpendicular (Faraday geometry) or parallel (Voigt geometry) to the growth axis of the 2D layers). The holder was positioned at the center of the field and was immersed in the cryogenic fluid or in an exchange gas. The power density on the sample usually did not exceed 2 mW/cm^2. The field values were monitored by a small calibrated pick-up coil imbedded in the plastic sample holder.

Experimental results and discussion

Undoped SQW in a Short-Pulse Magnet

We have studied two undoped AlGaAs-GaAs SQW samples in pulsed fields up to 65 T (6). The samples have well widths of 6 and 12 nm, respectively, and were measured at 4 and 77 K. At T=4 K and B=0 T, both samples displayed a single sharp excitonic peak due to the lowest e1-hh1 transition. At 77 K, two peaks were observed corresponding to the e1-hh1 and e1-lh1 transitions. In low fields (0-10 T), the peaks possess typical magneto-excitonic behavior with a characteristic diamagnetic shift (7). The line width (FWHM) increased with increasing field. In the high field regime, the shift became linear with increasing field. However, at about 25 T, the e1-hh1 and e1-lh1 transitions intersected and showed anticrossing. At 4 K, this was observed as a distinct change in the slope of the magneto-exciton energy and an increase in its line width. Above 30 T, the upper transition was observed when displayed on a logarithmic scale. Although the magneto-excitons are slightly broader at 77 K, the anti-crossing could be followed across the complete range of magnetic fields as shown in Fig 4 (a). The two peaks can be clearly resolved above and below the anti-crossing region. This observation of anti-crossing in high magnetic fields is thought to be related to valence band mixing effects of the heavy and light hole dispersion curves (9). Fig. 4 (b) shows a plot of transitions at 77 K. The solid line (4 K) and the dotted line (77 K) are calculated curves from which we obtain an exciton effective mass, $\mu^*=0.53m_0$ where m_0 is the electron rest mass. It can be seen that the 77 K dotted line initially follows the circular markers (e1-hh1) but at higher fields above 25 T, it follows the open-square markers (initially e1-lh1 at low fields). The dashed lines are guides to the eye to show the anti-crossing of the e1-hh1 and e1-lh1 transitions at 77 K. The calculated energy level in the conduction band, e1=61.7 meV and for the valence band hh1=16.8 meV; these values are in good agreement with the experimental measurements. From the MPL diamagnetic shift data, we estimate the dimensionality parameter, D to be 0.24 for the 6 nm well and 0.47 for the 12 nm well compared with the 3D and 2D limits where exact values for

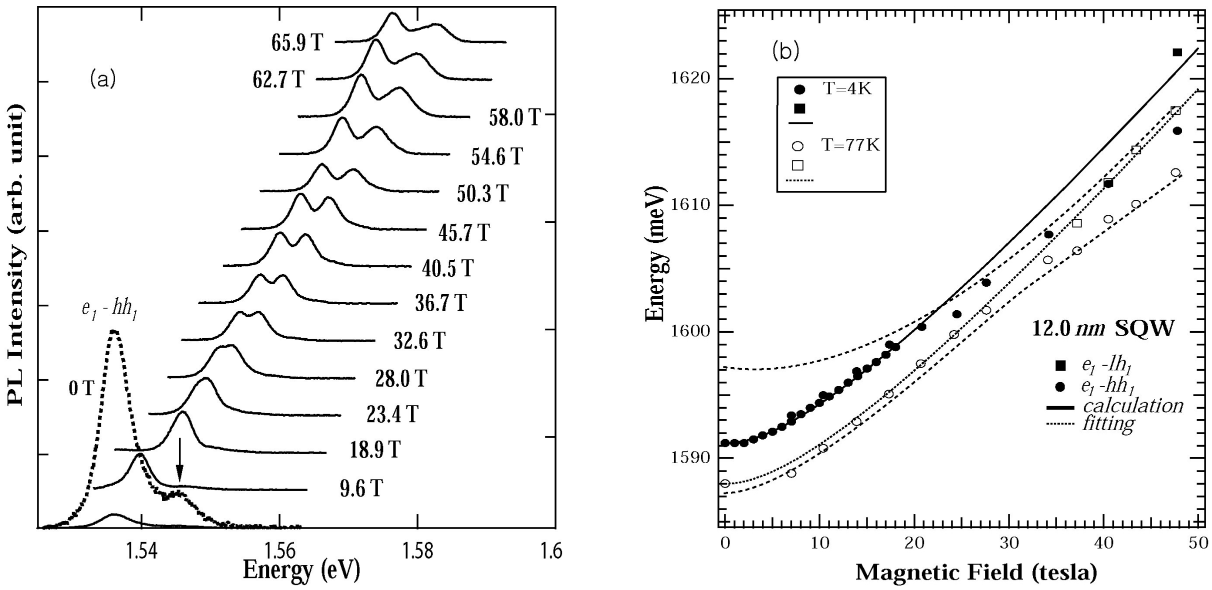

Fig 4. (a) PL spectra in 65 T short pulsed magnetic fields. (b) Energy vs. magnetic field plot. Solid circles and squares below 20 T indicate conduction band to heavy-hole transitions at 4 K and 77 K, respectively. Solid lines depict the simple diamagnetic transition behavior while broken lines depict anti-crossing behavior of heavy- and light-hole transitions

D_{3D}=1 and the D_{2D}=0.19. Our values are about a factor of two less than those reported by Rogers *et al* (7). for similar well widths and are closer to the 2D limit.

Modulation-doped SHJ in Magnetic Fields

The electric potential profile and the electronic structure of the sample used for this study are depicted in Fig 5. Due to the band bending which is occurred by modulation doping, the conduction band has wedge-shaped triangular quantum well with quantized energy levels (E0 and E1) whereas the valence band does not have confined energy levels. Consequently, photogenerated electrons near the flat band region move to the quantum well while the holes move the flat band region. We have performed magneto-transport measurement with and without laser illumination to a modulation doped single heterojunction in order to determine the density of two-dimensional electron gas (2DEG) in the quantum well. With increasing magnetic fields, the Fermi energy of the sample oscillates whenever the Landau levels cross the Fermi energy. This means that with increasing magnetic fields, electrons in a Landau level move down to the lower Landau levels and whenever a Landau level crosses the Fermi energy, it becomes completely empty. The

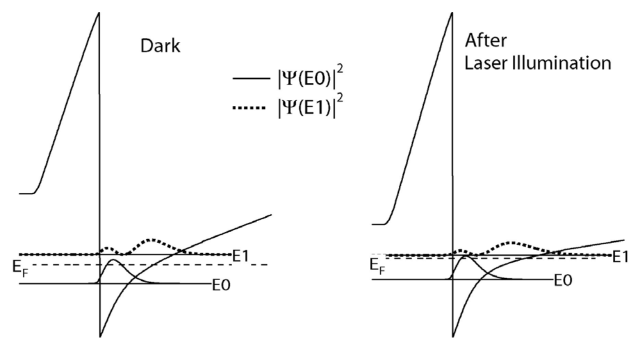

Fig 5. Calculated energy levels and wavefunctions. After laser illumination, as the potential well changed, the energy levels (E0, E1) and Fermi energy increased.

number of completely filled Landau level (Landau filling factor) is defined as,

$$\nu = N\frac{h}{eB} \tag{2}$$

where N density of 2DEG and h is Plank constant. During this process, the density of states at the Fermi energy oscillates that induces oscillation of resistance with the same period which is known as Shubnikov-de Hass (SdH) oscillations. The period of the SdH oscillation with respect to 1/B depends on the total density of electron. In Eq. 2, measuring magnetic field for ν=m (m is any integer number), the total 2DEG density (*N*) can be calculated as

$$N = \frac{e}{h} B_{\nu=m} \times m = \frac{B_{\nu=m} \times m}{4.14T} \times 10^{11} cm^{-2} \tag{3}$$

As seen in Fig 4 (a), ν=1 occurs at ~12 T, hence the density of 2DEG for this sample is $N=3\times10^{11}/cm^2$ without laser illumination. Since photoluminescence measurement is undertaken with high power laser illumination, it is impossible to determine the electron density due to the three dimensional carriers in the barrier which deteriorate the Shubnikov-de Hass oscillations. For this reason, we gradually increased the illuminated laser power while measuring SdH oscillations to determine the density while illuminating laser light. As the laser power gradually increased, the electron density increases as well. Further increasing laser power increases 3D carrier transport, it is difficult to find exact number of ν.

Fig 4 displays typical PL spectra of the SHJ sample taken at 4 K as a function of magnetic field for ***B***//**z** using generator-driven long pulse magnet. At *B*=0, the spectrum consists of three peaks located at 1515.5, 1514.0, and 1510.5 meV. The middle peak is the most intense and is related to the radiative excitonic recombination of the *E*1 subband with photocreated holes close to the top of the valence band in the GaAs layer. The higher-energy peak of medium intensity at 1514.0 meV is possibly due to the free exciton (FX) in bulk GaAs. The low-energy peak of weak intensity probably emanates from excitons bound to an ionized acceptor (A^{-}-*X*). The intensity of the FX peak and the A^{-}-*X* peak decrease with increasing magnetic field, and show a diamagnetic shift characteristic of excitonic transitions in the low field regime. Energy scans were taken at 0.2 ms intervals to 60 T. Intensity oscillations and small energy deviations (steps) from linear behavior for the *E*1 exciton transitions were observed over this magnetic-field range.

Before illuminating the sample with laser light, the electron density in the well is about 4.58×10^{11} cm^{-2}, and our theoretical calculation shows that the *E*0 and *E*1 energy levels and the Fermi energy lie at 47.7, 73.1, and 64.2 meV from the bottom of the well, respectively. The energy separation between the Fermi energy and the *E*1 subband is about 8.9 meV. After illuminating the sample, the electron density in the well increased to $5.82\times10^{11}cm^{-2}$, and the *E*0 and *E*1 energy levels change to 51.2 and 72.8 meV from the bottom of the well, respectively (see Fig 5). Another interesting result of our calculation is that the Fermi energy is located at 0.67 meV below the empty *E*1 subband. Due to this close proximity of *E*1 and the Fermi energy, strong Coulomb interaction between 2DEG and the excitons influence the magnetoexciton emission (8). The intensity modulation has the same period as the Shubnikov‐de Haas oscillation; this is in good agreement with Ref. 8.

In Fig 7, intensity minima occur when the Fermi energy is located in the extended states, whereas the energy maxima occur when the Fermi energy is located in the localized

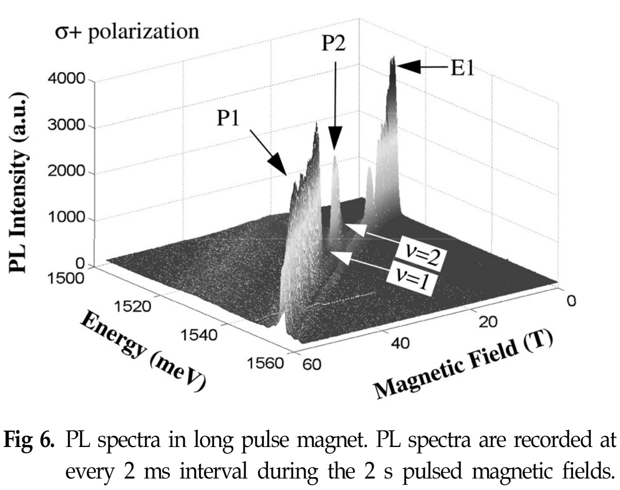

Fig 6. PL spectra in long pulse magnet. PL spectra are recorded at every 2 ms interval during the 2 s pulsed magnetic fields.

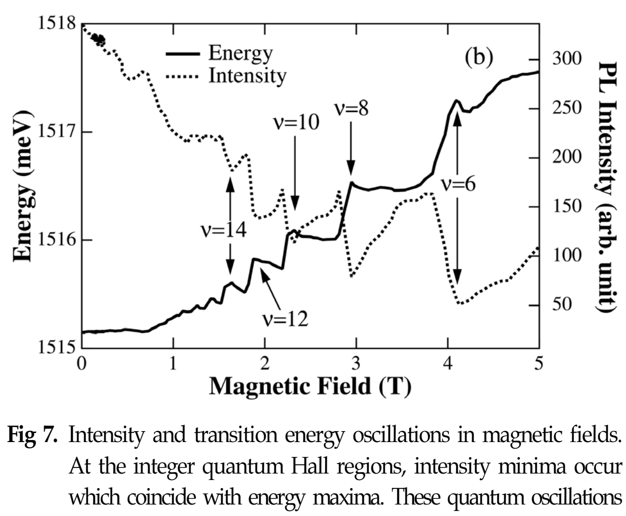

Fig 7. Intensity and transition energy oscillations in magnetic fields. At the integer quantum Hall regions, intensity minima occur which coincide with energy maxima. These quantum oscillations are due to the strong correlation within free carriers.

states. A Coulomb interaction between the 2D electron gas and the exciton state leads to the intensity modulation. When a Landau level of the 2D electron gas in the *E*0 subband crosses the *E*1 exciton state, due to a Coulomb interaction, corresponding eigenstates are hybridized. This enhances the interband matrix element for the overlapping transitions. When the Fermi energy crosses the *E*0 Landau levels, it changes the electron density in the *E*0 Landau levels that modulate Coulomb interactions between a 2D electron gas and an *E*1 exciton. This periodic change of the Coulomb interaction modulates the MPL intensity (8).

The nonlinear behavior of the transition energy is more complicated. When the Fermi level sweeps through an extended state, the screening strength changes because it is proportional to number of electrons in the Fermi level. Repeating this process with changing magnetic fields modulates the screening effect, which leads to a nonlinear behavior of the transition energy in an optical process. Hawrylak, Polsford, and Ploog (13) reported that energy oscillations can be eliminated by acceptor doping in a single heterojunction, while the PL intensity continues to oscillate with magnetic field. With acceptor doping, hole screening is negligible because holes in the valence band are blocked by the doped acceptors, and electrons can "see" only the acceptors. A theoretical study (9) also has shown that energy variation occurs at the even numbers of integer quantum Hall states due to the screened exchange and Coulomb hole self-energy. However, it is suggested that the Coulomb hole of the hole term is dominant, since the electron exchange and correlation are effectively canceled, and insufficient photocreated holes exist to make the hole exchange term.

In addition, we found a direct correlation between the SDH oscillations and the MPL data. The oscillations were approximately periodic with inverse magnetic field. Self-consistent Landau level calculations taking into account many-body interactions including Hartree and exchange- correlation potential were made (14, 15). The results of the calculations showed that both the population of the second subband, *E*1, and the energy gap between Landau levels from the *E*0 and *E*1 subbands undergo oscillations that are nearly periodic in inverse magnetic field. The calculated results are in good agreement with our experimental data and complement studies by Hawrylak *et al* (13). on a single heterojunction with a *p*-doped layer near the interface.

Pressure studies of a modulation-doped InGaAs-GaAs SQW

We have undertaken low temperature, pressure-dependent MPL measurements of an n-type modulation-doped $In_{0.2}Ga_{0.8}As/GaAs$ 8 nm-wide single-strained QW in DC (to 18 T) and pulsed (to 60 T) magnetic fields using a miniature diamond anvil cell (DAC). Landau level shifts were studied at 77 and 4 K with pressures ranging from ambient to about 30kb (Fig 8). The allowed 0-0, 1-1, 2-2, etc. Landau transition at 77 K were linear with magnetic field for all pressures. The pressure coefficients of the band-gap energy were in the expected 9~10 meV/kb range and were independent of magnetic field (19). At 4 K, only the allowed 0-0 transition dominated but forbidden transitions corresponding to 0-1, 0-2, etc. could be observed to about 18 T (the quantum limit for this

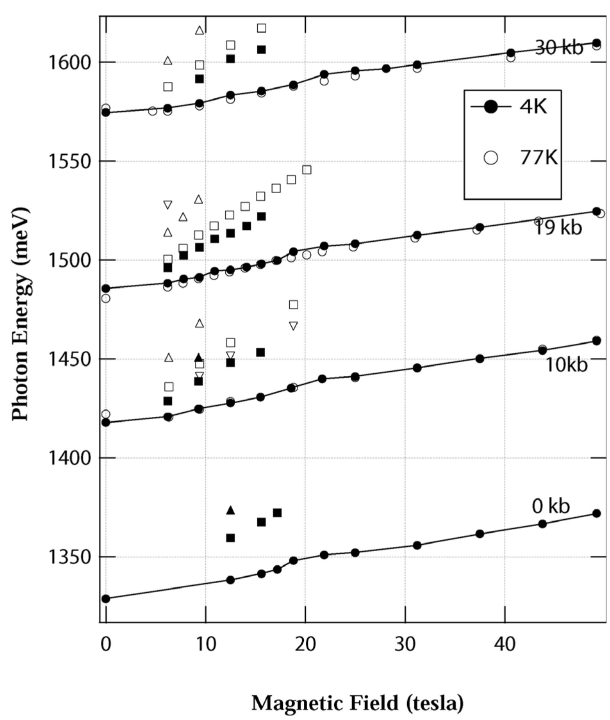

Fig 8. Transition energy vs. magnetic fields plot for various pressures in a diamond anvil cell (DAC). Even though the DAC has small aperture (~2mm), optical fiber technique allows to take PL spectra.

sample was estimated to be about 24 T). Variations in the Landau transition energies versus magnetic field and in the intensities occurred in the regions of ν=1, 2, 3,·····, similar to that observed in AlGaAs/GaAs modulation-doped QWs and SHJs (10-13). Near ν=1, the 0-0 transition showed a marked decrease in the slope with magnetic field from 25~60 T. Typical results are shown in Fig. 8 for measurements made at various pressure. Within the experimental error, the slopes of the Landau level transitions and the relative energy and intensity anomalies were independent of pressure. Above about 35 kb, the intensity of all the MPL Landau transitions rapidly diminished due to the influence of the Γ-X cross-over in the GaAs barrier and/or the InGaAs well.

Summary

Photoluminescence studies in pulsed magnetic fields to 65 T at low temperatures are established at NHMFL-LANL. We have undertaken a comprehensive investigation of magneto-excitonic and Landau transitions in a large variety of un-doped and modulation doped (2DEGs) QW heterostructures. In addition, we have demonstrated that it is possible to obtain high quality MPL spectral data on samples in a DAC at pressures up to ~4.0 kb at liquid helium temperatures. A He3 exchange gas cryostat allows optical studies to be made below 0.5 K in fields to 60 T. From undoped SQWs, we realized that heavy and light hole anticross at high magnetic fields above 25 T. For doped SHJ, strong correlation effects such as PL intensity and energy oscillations were observed in the presence of magnetic field. For the future works, one-dimensional quantum wire or nano-belt type low dimensional semiconductor heterostructures will be preferable, because reduced dimensionality might generate new correlations within free carriers. In addition, a capacitor-driven 50 T mid-pulse (~0.5 s) magnet system is under construction in the department of Applied Physics at Dankook University. The capacitor bank is consisted by 50 capacitors with total stored energy of 1.5 MJ. It will offer various physical measurements in ultra high magnetic fields such as optical spectroscopy, de Haas-van Alphen effect and magneto-transport.

References

(1) von klitzing K, Dorda G, Pepper M (1080) Phys Rev Lett **45**, 494

(2) Tsui DC, Störmer HL, Gossard AC (1982) Phys Rev Lett **48**, 1559.

(3) Heiman D (1992) In Seiler DG, Little CL Eds, Semiconductors and Semimetals, Vol. 36, Ch. 1, Academic Press, New York, p. 1 and references therein

(4) Lampart MA (1958) Phys Rev Lett **1**, 450.

(5) Stébé B, Ainane A (1989) Superlattices Microstruct **5**, 545

(6) Perry CH, Kim Y, Rickel DG (1995) In Fisk Z, Gorkov L, Meltzer D, Schrieffer R Eds "Physical Phenomena at High Magnetic Fields II" World Scientific, Singapore, p 97-102

(7) Rogers DC, Nicholas RJ, Foxon CT, Woodbridge K (1986) Phys Rev B **34**, 4002

(8) Kim Y, Perry CH, Lee K-S, Rickel DG (1997) Bull Am Phys Soc 42, 373

(9) Yang EYC, Sham L (1987) Phys Rev Lett **58**, 2598

(10) Perry CH, Worlock JM, Smith MC, Petrou A (1987) In Landwehr G Ed "High Magnetic Fields in Semiconductor Physics" Springer Series in Solid State Sciences, vol. 71, Springer, Heidelberg, p 202

(11) Goldberg BB, Heiman D, Pinczuk A, Pfei¤er L, West K (1990) Phys Rev Lett **65**, 641.

(12) Dahl M, Heiman D, Pinczuk A, Goldberg BB, Pfeiffer L, West K (1992) Phys Rev B **45**, 6957

(13) Hawrylak P, Pulsford N, Ploog K (1992) Phys Rev B **46,** 15193

(14) Lee KS, Lee EH (1994) J Appl Phys **76**, 5778

(15) Lee KS, Lee EH (1995) Phys Rev B **51**, 13315

(16) Kim Y, Perry CH, Rickel DG, Lee K-S (1996) Bull Am Phys Soc **41**, 240

(17) Kee K-S, Lee EH, Perry CH, Kim Y (1006) Inst Phys Conf Ser **145**, 459

(18) Jones ED, Dawson LR, Klem JF, Lyo K, Heiman D, Liu XC (1995) In Lockwood DJ Ed "Physics of Semiconductors" World ScientiFIc, Singapore, p 1492-1494.

(19) Jones ED, Lyo SK, Klem JF (1996) Int Phys Conf Ser **145**, 397

(20) Perry CH, Kim Y, Rickel DG (1998) Physica B **246,** 182

(Received Jan 15, 2007; Accepted Feb 25, 2007)